JBUON 2013; 18(4): 1074-1081
ISSN: 1107-0625, online ISSN: 2241-6293 • www.jbuon.com
E-mail: editorial_office@jbuon.com

ORIGINAL ARTICLE

Technetium-99m- Arg-Arg-Leu(g2), a modified peptide probe targeted to neovascularization in molecular tumor imaging

Xia Lu[1,2], Lingzhou Zhao[1], Tian Xue[1], Huabei Zhang[1]

[1]*Key Laboratory of Radiopharmaceuticals, Ministry of Education, College of Chemistry, Beijing Normal University, Beijing;* [2]*Medical Image Center, Beijing Aerospace Hospital, Beijing, China*

Summary

Purpose: *The ^{131}I-tRRL small peptide probe has been identified in our previous study as a robust tumor molecular radiopharmaceutical that specifically binds to tumor-derived endothelial cells. In this study we developed a smaller structure cyclic tRRL (g2) radiolabeled with ^{99m}Tc as a novel and optimized peptide probe on tumor angiogenesis molecular imaging.*

Methods: *Both tRRL (g2) and control peptide GGG (g2), as well as FITC-RRL (g2) and FITC-GGG (g2) peptide chains were synthesized and characterized by high performance liquid chromatography (HPLC) and electrospray ionization mass spectrometry (EMI-MS) analysis. After synthesis and purification, the peptides were radiolabeled with ^{99m}Tc by a one-step method for quantitative cell-binding assay and biodistribution experiments. A cell adhesion assay was performed to image tumor-derived endothelial cells-binding specificity with the novel RRL (g2) peptide probe in vitro. The biodistribution experiment was performed to show the tumor uptake of ^{99m}Tc-RRL (g2) compared with other tissues in human glioblastoma-bearing nude mice in vivo.*

Results: *FITC-RRL (g2) had significantly higher tumor-derived endothelial cell-binding affinity and specificity than the control FITC-GGG (g2). ^{99m}Tc-RRL (g2) had higher tumor uptake (2,578 ± 0.293 at 30 min postinjection) and longer tumor retention than ^{99m}Tc-GGG (g2) in the tumor models tested. The tumor specificity of ^{99m}Tc-RRL (g2) was also confirmed by successful quantitative cell binding experiments.*

Conclusion: *^{99m}Tc-RRL (g2) has more good characteristics such as higher tumor uptake ratio and short half life time compared with ^{131}I-tRRL. The information obtained here may guide the future development of RRL peptide-based tumor angiogenesis molecular imaging and internal radiotherapeutic agents targeting tumor neovascularity.*

Key words: *molecular imaging, peptide probe, RRL (g2), ^{99m}Tc, tumor angiogenesis*

Introduction

Tumor-induced angiogenesis is a pathological condition that results from aberrant deployment of normal angiogenesis, an essential process in which the vascular tree is remodeled by the growth of new capillaries from preexisting vessels. As a result of a large sum of metabolic demands of tumor tissue, tumor cells induce the formation of a new blood supply from the preexisting vasculature, and this makes tumor cells able to survive and propagate in a hostile environment [1]. The fact that tumor progression is dependent on angiogenesis has inspired scientists to search for novel imaging probes and optimize founded probes to trace tumor angiogenesis and to diagnose malignant tumors more earlier and monitor the clinical effects of treatment as well as cancer recurrence or metastasis. Among the available *in vivo* tumor angiogenesis molecular imaging modalities, nuclear imaging is the most powerful technique thanks to its visualization, characterization, and measurement of biological processes at the molecular and cellular levels in humans and other living systems and as molecular functional imaging modality [2].

Brown and colleagues identified the small peptide sequence motif of Cys-Gly-Gly-Arg-Arg-

Correspondence to: Huabei Zhang, PhD. No.19, xinjiekouwai St. West District, Beijing, 100875, China. Tel: +86 15810526188, E-mail: hbzhang@bnu.edu.cn
Received: 04/05/2013; Accepted: 28/05/2013

Leu-Gly-Gly-Cys (RRL) with binding specificity to tumor-derived endothelial cells (TDECs) by using of FliTrx™, a simplified peptide display library *in vitro* from SCC-VII murine squamous cell carcinomas. The peptide sequence is flanked by cysteine residues, which form a disulfide loop that constraints the expressed peptide RRL. This conformational constraint can improve binding of peptides to target molecules [3].

In our previous studies, we designed and synthesized decapeptide RRL by adding tyrosine to its amino terminal (Tyr-Cys-Gly-Gly-Arg-Arg-Leu-Gly-Gly-Cys), named tRRL, and then radiolabeling it with radioiodine-131 by the chloramine-T method. Biodistribution and SPECT imaging results indicated that ^{131}I-tRRL could accumulate specifically in tumor tissues in various tumor-bearing mice [4,5]. The development of tumor angiogenesis imaging and antiangiogenic agents has focused largely on the targeted site of vascular endothelial growth factor (VEGF) and VEGF receptors (VEGFRs) signal pipeline and integrins [6] that have pivotal role in tumor vasculogenesis. Then, we explored the association of tRRL to tumor cells and TDECs, and the possible relationship between tRRL and VEGFR-2. The results revealed that VEGFR-2, which is highly expressed on TDECs, was probably not the sole binding ligand for tRRL targeted to tumor angiogenic endothelium [7].

Although ^{131}I-tRRL was proved to be combined with TDECs and could accumulate and image tumor angiogenesis *in vivo* in various human cancer-bearing nude mice byγcamera as described in our previous study [5], however, ^{131}I-tRRL is not very suitable for clinical nuclear medicine imaging. Currently, nuclear medicine clinical use of probe for tumor angiogenesis imaging is mainly limited by the inherent properties of radioisotopes. Since ^{99m}Tc has many advantages compared with radioiodine 131, including an appropriate energy for imaging, a simpleγray emission and its physical halflife time is 6.02 d. What's more important priority is that ^{99m}Tc labeled radiopharmaceuticals have better image quality than ^{131}I. Our laboratories have been particularly interested in the probes of tumor angiogenesis imaging. In this study we report a novel peptide RRL(g2)(gly-gly-(D)Ala-gly-(D)ser-KCGRRLGC) modified from tRRL and radiolabeled by ^{99m}Tc as a more powerful angiogenesis imaging probe with promising properties in tumor angiogenesis molecular imaging.

Methods

Molecular docking

To locate the appropriate binding orientations and conformations, the RRL (g2) were docked into the VEGFR-2 binding pocket with the use of AutoDock4.0 software. Polar hydrogen atoms were added and the active torsions of ligand with Gasteiger partial charges, Kollman charges [6], atomic solvation parameters and fragmental volumes were assigned to the protein using AutoDock Tools (ADT). The grid maps around the active site were generated by the auxiliary program AutoGrid. The volume of the grid was set at 45×45×45 Å with a grid-spacing interval of 0.375 Å to cover the binding site. Lennard–Jones parameters 12-10 and 12-6, supplied with the program, were used for modeling van der Waals interactions and H-bonds, respectively. The electrostatic grid was calculated using the distance-dependent dielectric permittivity of Mehler and Solmajer. Lamarckian Genetic Algorithm (LGA) was performed for conformational search and the pseudo-Solis and Wets methods were applied for minimization using default parameters. The population in the genetic algorithm, the energy evaluations and the maximum number of iterations were 50, 250 000 and 27 000, respectively. The final structures were clustered and ranked according to RMS deviations and the lowest energy.

Synthesis of TDECs-Binding Peptide RRL (g2)

All chemicals used were of analytical grade and commercially available. The RRL (g2) peptide (Gly-Gly-(D)Ala-Gly-(D)ser-Lys-Cys-Gly-Arg-Arg-Leu-Gly-Cys-NH2) and the control peptide GGG (g2) (Gly-Gly-(D) Ala-Gly-(D)ser-Lys-Cys-Gly-Gly-Gly-Gly-Gly-Cys-NH2) were synthesized by the solid-phase peptide synthesis (SPPS) method using an Apex 396 Multiple peptide synthesizer (AAPPTEC, Louisville, USA), and disulfide bonds between cysteines on each peptide were formed to maintain the cyclic structure. The synthesis conditions used were: deprotection: 50% peperidine in DMF; coupling: coupling with amino acide/HOBt/DIC (2:2:1); cleavage: TFA/anisole/dimethylsulfide/ethanedithiol (91:3:3:3). The peptides were then purified by HPLC on a C18 column (4.6×250 mm) eluted with a gradient from 10 to 100% solvent A (0.05% trifluoroacetic acid in 2% acetonitrile) and 30 - 0% solvent B (0.05% trifluoroacetic acid in 90% acetonitrile at 1 mL/min, with monitoring at 220 nm). The lyophilized peptide was stored at -20 °C.

Radiochemistry properties studies

The reagents and solvents used in this study were purchased from commercial suppliers. Paper chromatography experiments were performed using 0.5 M phosphate buffer (pH 7.4) and #1 filter paper (Xinhua). Reversed-phase HPLC was performed on a system with an LC-20AT pump (Shimadzu Corp.). The C-18

reverse-phase semipreparative HPLC column (10×250 mm, 5-mm particle size [Venusil MP-C18; Agela Technologies Inc.]) was eluted at a flow rate of 5 ml/min. In brief, a solution of peptide RRL (g2) and GGG (g2) was prepared at a concentration of 2 mg/ml in 0.5 M phosphate buffer (pH 7.4). A fresh 5 μg (0.5 mg/ml) stannous chloride, 0.5 M phosphate buffer and ^{99m}TcO4- were added in the solution of the peptides. This reaction mixture was incubated at room temperature for 15-30 min. Then, the reaction mixture was injected onto a semi-HPLC column for purification. The column was eluted with TFA 0.05%+CH3CN 2% (solvent A) and TFA 0.05%+CH_3CN 90% (solvent B) at a flow rate of 5.0 ml/min. The gradient was 90% A from 0 to 5 min, 90–85% A from 5.01 to 10 min and 85–75% A from 10.01 to 15 min. The desired product was collected from the HPLC column, and the solvent was evaporated using a rotary evaporator. The product was redissolved in 0.9% saline and filtered through a 0.22-mm Millipore filter. The final radiochemical purity was determined by reinjection of the product onto a radio-HPLC column, and the radioactive fraction was collected and measured in a dose calibrator for specific activity calculation. In order to measure the stability of the probe, the ^{131} I-RRL (g2) (37KBq, 10 μl) was incubated in saline (1ml) at 4 ^{0}C and at room temperature for 4h, and in human serum (1ml) at room temperature and 37 ^{0}C for 4h; then their radiochemical purity was measured.

Cell lines

For cell culture experiments, human umbilical vein endothelial cells (HUVECs) were cultured in growth factors containing ECM medium with 5% fetal bovine serum (ScienCell, USA), and human glioblastoma cells U87 (American Type Culture Collection) were grown in low sugar DMEM medium (Invitrogen, USA) with supplementation of 10% fetal bovine serum, penicillin (100 U/ml), and streptomycin (100 mg/ml). All cells were cultured in a humidified atmosphere with 95% air and 5% CO_2 at 37 ^{0}C. The experiments were performed with cells in the logarithmic phase of growth.

Cell adhesion assay and binding experiment

For confocal microscopy, 4-6×10^5 HUVEC cells were seeded into chamber slides (Thermo Fisher Scientific, USA) and cultured overnight. The medium was removed and the cells were incubated with FITC-RRL (g2) and the control peptide FITC-GGG (g2) (5 μg/ml) in 400 μl fresh medium for 30, 60, 120, and 240 min at 37 ^{0}C. Cells were rinsed 3 times with PBS at room temperature. After 3 rinses with PBS, the cells were fixed with 3.7% paraformaldehyde for 30 min. The slides were mounted in Vectashield containing 4,6-diamidino-2-phenylindole (DAPI) (Vector Laboratories Inc., USA) and kept at 4 ^{0}C overnight. Images were taken with an inverted LSM510 confocal microscope (Carl Zeiss, Germany) at the Advanced Optical Microscopy Center of Life Science College (Beijing Normal University). Excitation was at 364 and 490 nm for visualization of DAPI and FITC, using 385 to 470 nm and 525 nm emission filters, respectively. Images were analyzed using LSM-Viewer software (version 3.5.0.376; Carl Zeiss, Germany).

HUVECs were cultured in 24-well plates (5×10^4 per well). Cells were starved for 16 h in serum-free medium, then cocultured with medium containing 37 kBq ^{99m}Tc-RRL (g2) and ^{99m}Tc-GGG (g2) per well. We harvested the medium (non-uptake tracer) and cells (uptake tracer) of each well at 30, 60, 120, and 240 min, and radioactivity was measured using a γ-well counter along with a standard (treatment for each well was repeated 3 times). The binding ability of ^{99m}Tc-RRL (g2) and ^{99m}Tc-GGG (g2) was represented by the ratio of mean uptake. Uptake ratio = uptake counts / mean total counts (uptake and non-uptake counts) ×100%.

Animal models

Animal procedures were performed according to a protocol approved by the Institutional Administrative Panel on Laboratory Animal Care of Beijing Normal University. The U87 glioblastoma xenograft model was generated by subcutaneous injection of 1×10^7 U87 cells (VEGFR and integrin $\alpha_v\beta_3$ positive) into the front left flank of male athymic nude mice. Two to 3 weeks after inoculation (tumor diameter 0.4-0.5 cm), the mice were used for biodistribution study.

Biodistribution study

About 185 kBq of ^{99m}Tc-RRL(g2) and ^{99m}Tc-GGG(g2) in 0.1 ml sterile PBS solution were injected through the tail vein of human glioblastoma-bearing nude mice (N=5 in each group). All 40 injections were tolerated well. The mice were sacrificed at 30 min, 1, 3, and 6 h post injection, and the tissues and organs of interest were collected, weighed wet, and counted in a γ-well counter. The percentage of the injected dose per gram (ID/g %) for each sample was calculated by comparing its activity with an appropriate standard of the injected dose. The values were expressed as mean ± SD.

Statistics

The data were expressed as means ± standard deviation (SD). Student's t-test and one-way ANOVA test were used for statistical evaluation. A $p < 0.05$ was considered statistically significant.

Results

Molecular docking

Since the molecular docking of tRRL has been reported in our previous study, smaller ring of RRL (g2) was positioned in the active site of

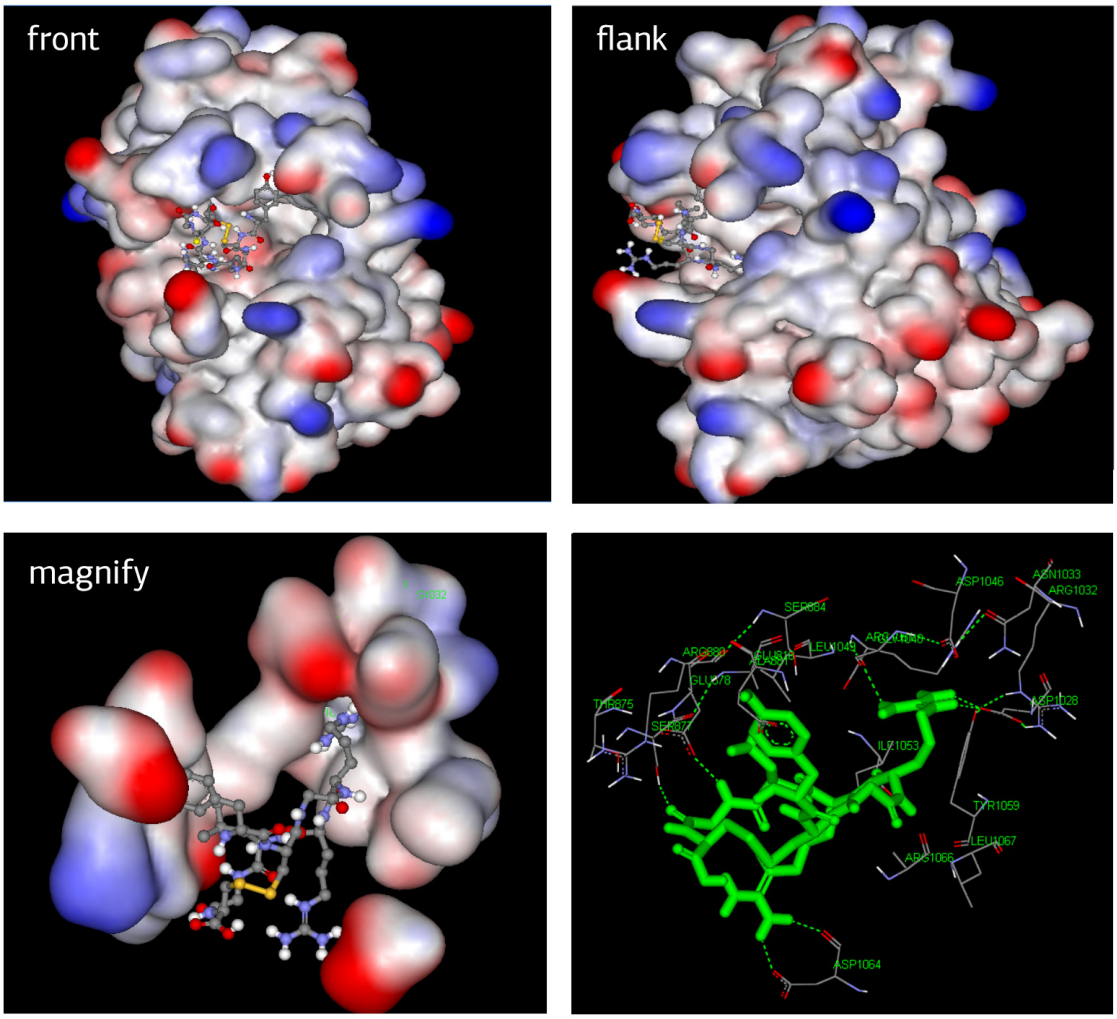

Figure 1. Different views of the docked RRL(g2) in the active pocket of VEGFR-2 .

VEGFR-2 into the binding pocket. The structure of RRL (g2) was more suitable for the gorge at the active site than tRRL. As shown in Figure 1, molecules after docking adopted the reasonable conformations and no collision with the active pocket occurred. The autodocking energy was 6.06 compare to 6.89 of RRL.

Chemistry

The nonradioactive peptides RRL (g2), GGG (g2), FITC-RRL (g2) and FITC-GGG (g2) were synthesized and reversed-phase HPLC of the crude product yielded a main peak containing over 99% of the absorbance at 220 nm (Figure 2).

Radiochemistry properties

The overall decay-corrected radiochemical yields were 73% ±7.4% and 70%±6.8% for ^{99m}Tc-RRL (g2) and ^{99m}Tc-GGG (g2), respectively. The radio-HPLC retention times of ^{99m}Tc-RRL (g2) and ^{99m}Tc-GGG (g2) were 5.7 and 5.5 min, respectively. The radiochemical purities calculated from radio-HPLC chromatograms of both tracers were more than 95% after purification.

After storage in human plasma at 37 ^{0}C for more than 4 h, about 93% intact product of ^{99m}Tc-RRL (g2) were eluted from HPLC. When stocked in 0.9% saline solution, the tracers were stable during at least a 4-h period. Therefore, the HPLC-purified tracers were best stocked in 0.9% saline solution first (Figure 3).

Ex vivo cell adhesion and binding assay

We observed that HUVECs were stained with FITC-RRL (g2) in cytoplasm and nuclei as soon as cocultured for 30 min, but not with FITC-GGG (g2). When cocultured over 2 h, both FITC-RRL (g2) and FITC-GGG (g2) were adhered abundantly in HUVECs (Figure 4). In quantitative cell binding assay, the uptake ratio of ^{99m}Tc-RRL (g2) in HUVECs was nearly 3-fold higher ($p<0.05$) than ^{99m}Tc-GGG (g2) uptake (Figure 5).

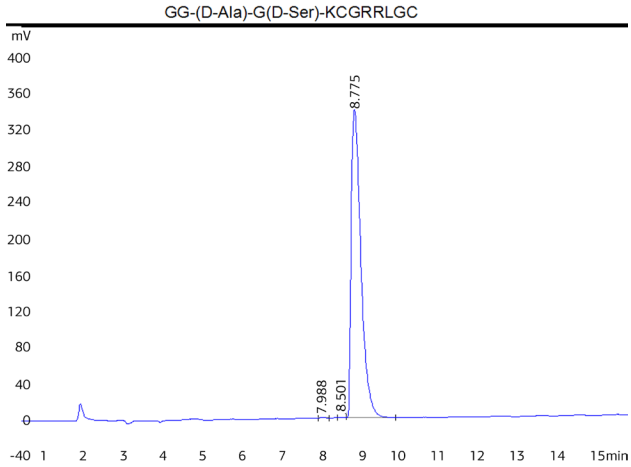

Figure 2. Schematic structure of RRL(g2) peptide (top) and reversed-phase HPLC of RRL(g2) peptide (bottom).

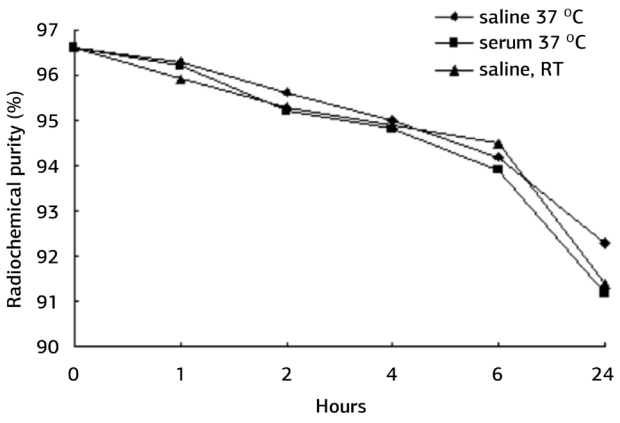

Figure 3. The radiochemical purity of ^{99m}Tc-RRL(g2) was over 90% at room temperature (RT), in normal saline at RT, and in fresh 37 °C human serum at 0.01 mg/mL for 24h, respectively.

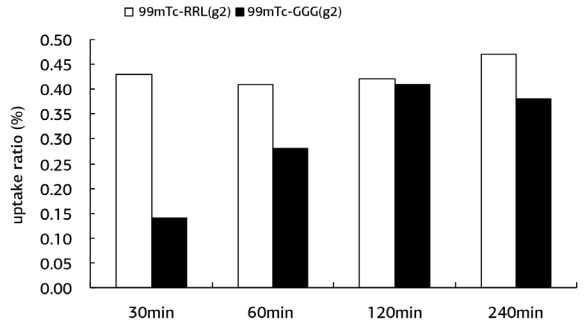

Figure 5. Uptake ratio of ^{99m}Tc-RRL(g2) and ^{99m}Tc-GGG(g2) by HUVECs. The uptake ratio of ^{99m}Tc-RRL(g2) was increased with prolonged incubation time. Conversely, the uptake ratio of ^{99m}Tc-GGG(g2) was lower within one hour compared with RRL(g2).

Biodistribution in mice

The biologic distribution results in mice are shown in Table 1 and Table 2. Both ^{99m}Tc-RRL (g2) and ^{99m}Tc-GGG (g2) had high initial liver, kidney, stomach and tumor uptake (3.144±1.016 , 8.047±0.519, 6.926±0.627 and 2.758±0.293 ID%/g at 30 min post injection, respectively). Meanwhile, uptake in most other tissues was also high, especially in spleen and lung, resulting in low tumor-to-nontarget ratios for both tracers at 30 min post injection. However, tumor uptake was still high but other tissues' uptake of the tracer became low in the ^{99m}Tc-RRL (g2) group 6 h post injection, but not in the ^{99m}Tc-GGG (g2) group. As described in Table 1, ^{99m}Tc-RRL (g2) had high initial tumor uptake and cleared slowly; about 15% of the tracer was eliminated from the tumor during 6 h post injection (2.342±0.404 ID%/g 6 h post injection). Compared with ^{99m}Tc-RRL (g2), ^{99m}Tc-GGG (g2) had more quick clearance from the tu-

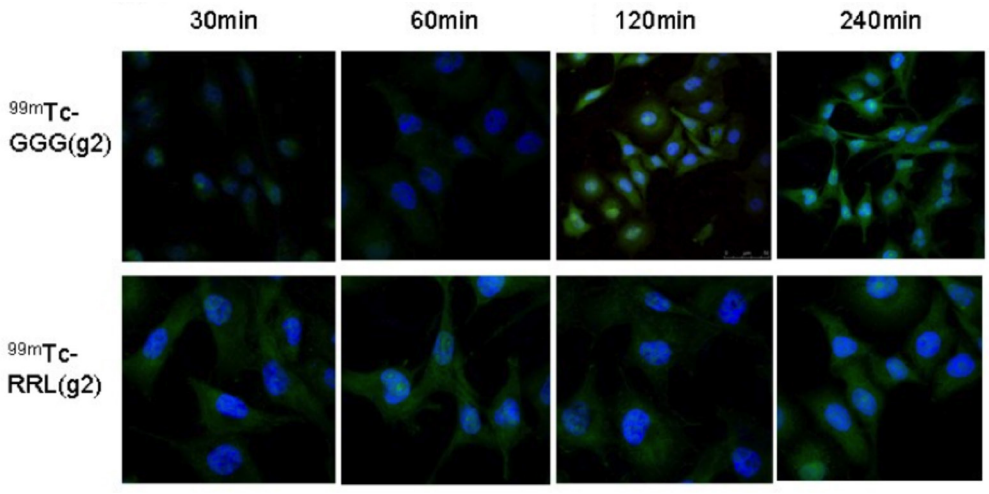

Figure 4. FITC-GGG(g2) and FITC-RRL(g2) binding to HUVEC cells after coculture for different times.

Table 1. Distribution on results ^{99m}Tc-RRL (g2) in glioma bearing nude mice

Tissue	*Postinjection time (h)*			
	0.5	*1*	*3*	*6*
Heart	2.755±0.541	1.945±0.586	1.312±0.969	1.381±0.144
Liver	3.144±1.016	2.898±0.550	1.739±0.538	1.065±0.299
Spleen	2.675±1.137	1.933±0.130	1.820±0.197	1.451±0.109
Lung	2.761±0.764	2.526±0.190	1.873±0.026	1.48±0.146
Kidney	8.047±0.519	6.122±0.283	6.055±0.331	3.393±0.218
Stomach	6.926±0.627	5.479±0.570	4.287±0.089	3.857±0.333
Small intenstine	1.982±0.079	1.645±0.504	1.349±0.446	1.075±0.253
Bladder	2.098±0.932	1.845±0.747	1.077±0.271	0.836±0.091
Skeletal muscle	1.572±0.310	1.362±0.348	0.347±0.102	0.229±0.055
Bone marrow	1.496±0.159	1.334±0.248	0.297±0.086	0.236±0.094
Tumor	2.758±0.293	2.675±0.503	2.526±0.280	2.342±0.404
Blood	2.008±0.350	1.827±0.159	0.963±0.252	0.542±0.277

Data are %ID/g±SD (N=5)

Table 2. Distribution on results ^{99m}Tc-GGG (g2) in glioma bearing nude mice

Tissue	*Postinjection time (h)*			
	0.5	*1*	*3*	*6*
Heart	2.167±0.750	2.150±0.457	1.267±0.185	1.090±0.170
Liver	3.810±1.288	2.380±0.494	2.273±0.560	1.930±0.438
Spleen	2.000±0.347	1.803±0.587	1.183±0.309	0.815±0.092
Lung	2.587±0.481	1.810±0.618	1.150±0.491	0.925±0.163
Kidney	8.020±0.830	7.867±0.129	5.570±0.291	3.600±0.042
Stomach	6.41±0.190	6.110±0.439	4.967±0.271	3.130±0.636
Small intenstine	1.823±0.217	1.330±0.244	1.217±0.179	1.395±0.064
Bladder	1.737±0.561	1.653±0.293	1.173±0.112	0.405±0.007
Skeletal muscle	1.483±0.527	1.143±0.179	0.860±0.21	0.290±0.028
Bone marrow	1.490±0.311	1.157±0.087	0.753±0.393	0.300±0.028
Tumor	2.267±0.375	1.573±0.501	1.233±0.409	0.780±0.099
Blood	2.420±0.272	2.220±1.039	1.447±0.331	0.370±0.141

Data are %ID/g±SD (N=5)

mor (0.78±0.099 ID%/g 6h post injection;Table 2), leading to high tumor-to-nortarget ratios in the ^{99m}Tc-RRL (g2) group. Both tracers had high initial kidney and stomach uptake, suggesting the tracers may be excreted mainly via the kidney.

Discussion

In this proof-of-principle study, we have demonstrated that tumor angiogenic vessels can be visualized by targeted nuclear technological imaging using the small peptide probe ^{99m}Tc-RRL(g2) targeted to tumor-derived endothelial cells. These data have implications for the development of small peptides as a novel targeted molecular imaging probe for noninvasive imaging of tumor angiogenesis with SPECT/CT.

Targeted nuclear medicine imaging is currently being evaluated for the visualization of tumor angiogenesis with the use of various radionuclides with different properties, conjugated to various types of targeted ligands that bind to special molecular markers of angiogenesis, including VEGFR2, endoglin, or integrins [8]. In this work, we tested whether RRL(g2) peptides could be used as a new class of endothelial-binding ligands for targeted nuclear molecular imaging of tumor angiogenesis, with the idea that, if successful, this study would provide proof-of-concept for engineering small peptides against biologic markers of angiogenesis.

In our previous study [4], we redesigned and radiolabeled tRRL with iodine-131 successfully and observed good imaging effects *in vivo* in tu-

mor functional SPECT imaging. In this report, we modified tRRL and shrink the cyclic structure by getting rid of two glycines to increase its tumor uptake ratio. We further explored the radiolabeling protocol of ^{99m}Tc-RRL (g2) by adding the sequence of (D) Ala-Gly-Gly-Lys which can anchor the technetium-^{99m} by its ring structure.

Noninvasive imaging strategies for the detection and quantification of tumor angiogenesis may be particularly helpful for diagnosing cancer at early stages, developing anticancer therapeutic agents in preclinical animal models, and monitoring antiangiogenic and tumoricidal treatments in cancer patients [9]. The development of tumor angiogenesis imaging and antiangiogenic agents has focused largely on the targeted site of VEGF and VEGF receptors signal pipeline and integrins [6] that has pivotal role in tumor vasculogenesis. A number of strategies has been used to inhibit the biologic activity of VEGF, including antibodies to the cytokine or its signaling receptor [10], receptor tyrosine kinase inhibitors [11–13], and gene therapy approaches, in which the vector produces an antisense molecule or a soluble receptor that acts in a dominant negative manner [14]. Because of their small size, these peptide probes can be produced by solid-phase synthesis, allowing chemical handles to be introduced for site-specific conjugation to the many traces such as macrobubbles, radionuclides, superparamagnetic particles, green fluorescence protein and nanoparticles and so on. But there is limited experience in using novel peptides as binding ligands to assess tumor angiogenesis *in vivo*.

RRL (g2) peptides are small peptides that consist of a core of at least 2 disulfide bonds cyclized into a ''ringlike'' conformation. RRL (g2) have great potential for *in vivo* applications due to their resistance to proteolysis and their high thermal stability. In addition, this class of molecules is thought to be nonimmunogenic [15].

The cell adhesion assay and binding experiment *in vitro* indicated that ^{99m}Tc or FITC targeted via RRL (g2) selectively bound to TDECs but not the control glycine peptide GGG (g2) under physiologically relevant shear conditions within 30 min, suggesting specific binding interactions between the RRL (g2) sequence and its ligands on the endothelial surface. ^{99m}Tc or FITC conjugated to GGG (g2) showed increased adherence to TDECs with the prolonged cocultured time, indicating a degree of nonspecific adhesion by the cyclic peptide. The biodistribution of ^{99m}Tc-RRL (g2) *in vivo* was characterized by quick blood clearance, with 2.008 ID%/g remaining 30 min after injection and 0.542 ID%/g remaining at 6 h. On the contrary, the uptake of tracer in tumors was detained, with 2.758 ID%/g remaining 30 min after injection and 2.342 ID%/g remaining at 6 h (about 15% of the tracer was cleared in 5 h). The ratio of tumor-to-blood was significantly different between groups, in particular the highest ratio value appeared at 6 h. The fast blood clearance and high tumor uptake were similar to the results on cyclic RGD radiolabeled with ^{99m}Tc, which is integrin αvβ3-specific and widely used in integrin expression imaging [16].

The small molecular size of ^{99m}Tc-RRL (g2) may be attributed to its fast blood clearance. However, the interaction between RRL (g2) and TDECs examined by cell binding assay and biodistribution experiment showed prominent initial uptake in tumor vascular cells and much longer tumor retention, presumably because of the optimal receptor-binding affinity/selectivity and adequate contact with the binding pocket located in the TDECs. The mechanism underlying such a phenomenon remains to be elucidated.

Both RRL (g2) and GGG (g2) exhibited higher gastric and renal uptake in different time points which might be caused by the overall difference in molecular charge. We noticed that even though the uptake of ^{99m}Tc-RRL (g2) in the stomach and kidney was high, no appreciable activity was excreted to the urinary bladder over time. Such a phenomenon suggests that receptor-mediated binding might be involved. VEGF and integrins play important roles in gastric and renal development. VEGFR and integrin αvβ3 are expressed in the gastric and renal endothelia of adults and, to a lesser extent, in all tubular epithelia [6]. The trend of increased kidney uptake from RRL (G2) would thus be due, in part, to the increased ligand-binding affinity and the molecular size.

It is important to have high tumor-to-kidney ratios, as well high absolute tumor uptake and longer retention, for both imaging and therapeutic applications. For imaging purposes, renal accumulation of radiolabeled peptides will reduce the sensitivity of detection in the vicinity of the kidneys. For therapeutic applications, renal accumulation of radiolabeled peptides limits the maximum tolerated doses that can be administered without inducing radiation nephrotoxicity. Thus, further modification is needed to improve the pharmacokinetics of RGD peptide-based radiopharmaceuticals.

Acknowledgements

This work supported by China post doctoral Science Foundation (2012M520187) and the Capital Health Development Scientific Research Funds (2011-6032-03).

References

1. Michael P, Iram H. Mechanisms of normal and tumor-derived angiogenesis. Am J Physiol Cell Physiol 2002;282:C947–C970.
2. Mankoff DA. A definition of molecular imaging. J Nucl Med 2007;48:18N-21N.
3. Brown CK, Modzelewski RA, Johnson CS, Wong MK. A Novel Approach for the Identification of Unique Tumor Vasculature Binding Peptides Using an E.coli Peptide Display Library. Ann Surg Oncol 2000;7:743–749.
4. Yu MM, Wang RF, Yan P et al. Design, synthesis and iodination of an Arg-Arg-Leu peptide for potential use as an imaging agent for human prostate carcinoma. J Label Compd Radiopharm 2008;51:374-378.
5. Lu X, Yan P, Wang RF et al. The further study on radioiodinated peptide Arg-Arg-Leu targeted to neovascularization as well as tumor cells in molecular tumor imaging. J Radioanalyt Nucl Chem 2011;290:623-630.
6. Waerzeggers Y, Monfared P, Viel T et al. Specific biomarkers of receptors, pathways of inhibition and targeted therapies :pre-clinical developments. Br J Radiol 2011;84:S168-S178.
7. Lu X, Yan P, RF et al. Use of Radioiodinated Peptide Arg- Arg-Leu Targeted to Neovascularization as well as Tumor Cells in Molecular Tumor Imaging. Chin J Cancer Res 2012;24 :52-59.
8. Nyberg P, Xie L, Kalluri R. Endogenous inhibitors of angiogenesis. Cancer Res 2005;65:3967–3979.
9. Buscombe JR, Wong B. PET a tool for assessing the in vivo tumour cell and its microenvironment? Br Med Bull 2013 ;105 :157-167.
10. Ferrara N. VEGF and the quest for tumor angiogenesis factors. Nat Rev Cancer 2002;2 :795-803.
11. Cai W, Chen X. Anti-angiogenic cancer therapy based on integrin avb3 antagonism. Anticancer Agents Med Chem 2006;6:407–428.
12. Gwyther SJ. New imaging techniques in cancer management. Ann Oncol 2005;16:ii63–ii70.
13. Rudin M, Weissleder R. Molecular imaging in drug discovery and development. Nat Rev Drug Discov 2003;2:123–131.
14. Jain RK. Physiological barriers to delivery of monoclonal antibodies and other macromolecules in tumors. Cancer Res 1990;50:814–819.
15. Willman JL, Murugan P, Chen K et al. US Imaging of Tumor Angiogenesis with Microbubbles Targeted to Vascular Endothelial Growth Factor Receptor Type 2 in Mice. Radiology 2008;245:508-518.
16. Fani M, Psimadas D, Zikos C et al. Comparative evaluation of linear and cyclic 99mTc-RGD peptides for targeting of integrins in tumor angiogenesis. Anticancer Res 2006;26:431-434